Proc. Indian Acad. Sci. (Chem. Sci.), Vol. 103, No. 3, March 1991, pp. 211–224.

Sub-Doppler laser spectroscopy of molecules and clusters in cold beams

F BYLICKI, W DEMTRÖDER*, H A ECKEL, J GRESS, E MEHDIZADEH and G PERSCH
Fachbereich Physik, Universität Kaiserslautern, D-6750 Kaiserslautern, Germany

Abstract. This paper illustrates, with several examples, the spectral resolution and attainable sensitivity reached with sub-Doppler laser spectroscopy in cold argon beams, seeded with molecular or metal vapors. Linear as well as nonlinear spectroscopy has been applied. The detection techniques use either LIF or resonant two-photon ionization. Examples given include NO_2, SO_2 and Na_3-molecules. The advantage of optical double resonance methods is illustrated.

Keywords. Sub-Doppler laser spectroscopy; molecular beams; two-photon-ionization; saturation spectroscopy; optical double resonance.

1. Introduction

The two main experimental methods for investigations of molecular structure and molecular interactions have been based on measurements of cross-sections for collisions in crossed atomic or molecular beams or on molecular spectroscopy. The combination of molecular beam techniques with different methods of high resolution laser spectroscopy has imparted remarkable impetus to molecular physics. Examples are the elucidation of congested molecular spectra by drastic reduction of the line density in cold supersonic beams or the formation and spectroscopic investigation of loosely bound van der Waals-molecules or of atomic and molecular clusters.

The advantages of molecular beams for the progress of spectroscopy can be attributed to the following facts:

(1) The reduction of the Doppler width in collimated beams, thus allowing sub-Doppler resolution.
(2) The simplification of molecular spectra by adiabatic cooling of molecules in supersonic beams.
(3) The realization of collision-free conditions for measurements of lifetimes of selectively excited molecular levels and for the study of free Rydberg molecules.
(4) The possibility of nonlinear laser spectroscopy and optical double resonance techniques in collimated cold molecular beams, where in favourable cases the spectral resolution is only limited by the transit time of the molecules through the radiation field.

Owing to the fascinating aspects of these combined techniques very active research

* For correspondence

has developed in many laboratories. The examples given in the present paper are mainly taken from recent work in Kaiserslautern. They represent of course only a small fraction of this rapidly expanding field of laser spectroscopy (Demtröder 1982; Scoles 1988/1989).

2. Sensitive detection methods

For sub-Doppler laser spectroscopy in a collimated molecular beam the laser beam intersects the molecular beam perpendicularly at a distance z_0 downstream of the nozzle (figure 1).

Due to the low molecular density in the beam and the short absorption path length Δx the absorption $\alpha(\omega_0)\cdot\Delta x$ may be below 10^{-10}. Therefore sensitive detection methods are necessary to monitor the absorption spectrum. A well known technique is excitation spectroscopy where the total fluorescence $I_{Fl}(\omega)$ emitted by the laser excited molecules is monitored while the laser frequency ω is scanned (figure 2a). The signal rate, given by the number n_{Ph} of photoelectrons per second at the exit of the photomultiplier

$$n_{Ph} = N_i \cdot n_L \cdot \sigma_{ik} \cdot \eta_{Ph} \cdot \delta \cdot \Delta x, \tag{1}$$

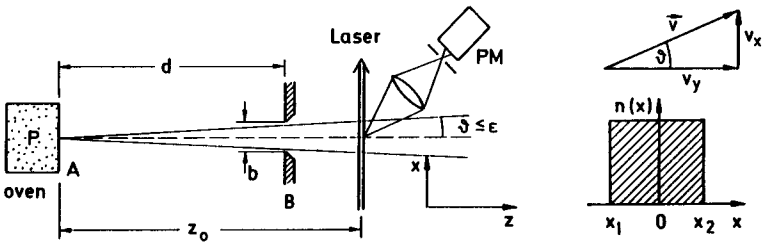

Figure 1. Sub-Doppler laser excitation spectroscopy in a collimated molecular beam.

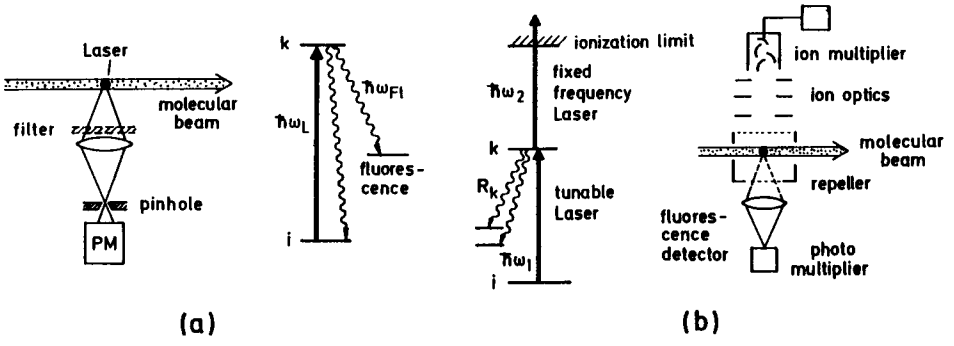

Figure 2. Level scheme for excitation spectroscopy (**a**) and resonant two-step photo-ionization (**b**).

is given by the density N_i of absorbing molecules in level $|i>$, the flux n_L of laser photons, the absorption cross section σ_{ik}, the collection efficiency δ, the quantum efficiency η_{Ph} of the photomultiplier cathode, and the absorption path length Δx. With a special design for collecting the fluorescence, which consists of an elliptical and a spherical mirror with high-reflecting coatings imaging the emitting volume into an optical fiber bundle (figure 2), collection efficiencies δ of up to 80% can be achieved (Gottwald 1985). The quantum efficiency η_{Ph} can reach 15%. Inserting these figures into (3) shows that at incident laser powers of 100 mW relative absorptions

$$\alpha \cdot \Delta x = N_i \sigma_{ik} \Delta x = n_{Ph}/(n_L \cdot \delta \cdot \eta_{Ph} \cdot \eta_K)$$

of $\alpha \cdot \Delta x \leqslant$ less than $5 \cdot 10^{-15}$ can still be detected at a rate of $n_{Ph} \leqq 100$ photoelectrons per second.

Instead of detecting the fluorescence photons, the excited molecules can also be ionized by a second laser (figure 2b). If this laser is sufficiently intense to ionize the excited molecules *before* they decay by fluorescence, each absorbed photon $h\nu_1$ of the first laser is converted by the second laser into an ion plus a photoelectron, which can be collected by an electric field and accelerated onto the cathode of an open particle multiplier. With pulsed lasers this resonant two-photon ionization represents the most sensitive detection method. The pulse width of dye lasers pumped by Nd-YAG-lasers or excimer-lasers is about 10 ns and therefore comparable or shorter than the radiative lifetimes of most molecular states. With the available high peak powers nearly every excited molecule can be photoionized without focussing the laser. Due to the short pulse duration, the diffusion of excited molecules out of the ionization volume can be completely neglected.

Although the detection efficiency during the laser pulse approaches 100%, the resonant two-photon ionization with pulsed laser in a cw molecular beam can *not* detect all molecules in the absorbing level $|i\rangle$. At a laser pulse width of 10 ns and a typical repetition rate of $\leqslant 100$/s the duty cycle is only $\leqslant 10^{-6}$! This means that most molecules passing through the interaction region in between two successive pulses escape detection. Pulsed lasers are therefore a good choice in combination with *pulsed* molecular beams. For cw molecular beams either pulsed lasers with a very high repetition rate can be used (e.g. copper vapor laser-pumped dye lasers) where the laser beams are sent along the molecular beam axis or cw-lasers, which are more appropriate.

With single-mode cw lasers a much higher spectral resolution can be reached. However, the experimental situation is more difficult. In order to reach the high intensities necessary for efficient photoionization, the laser beams must be focussed. However, the excited molecules travel during their lifetime of about 10 ns only 5 μm at thermal velocities of $5 \cdot 10^4$ cm/s. The focus of the ionizing laser beam must therefore coincide with that of the exciting laser within these tolerances. An experimental realization which meets this requirement is shown in figure 3. The light of the two lasers is transmitted to the experiment through two single mode optical fibers with 5 μm core diameter each. The two fiber ends are held closely together and the divergent output beams are collected by a common spherical lens and focussed by a cylindrical lens to form two thin "sheets of light" with the focal line perpendicular to the axis of the molecular beam. By turning the two fiber ends, the two focal lines can be shifted against each other thus optimizing the overlap, which can be monitored by

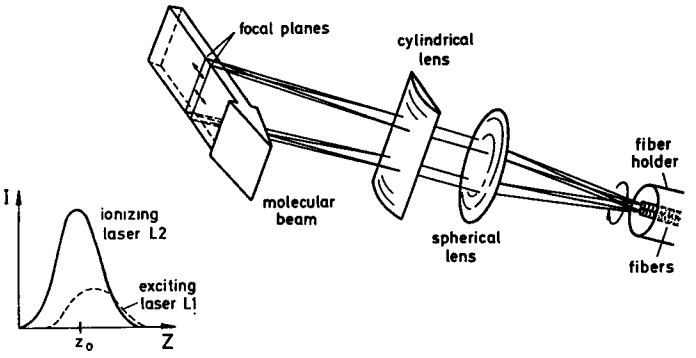

Figure 3. Resonant two-step photo-ionization. Experimental arrangement for two cw lasers.

maximizing the ion signal (Demtröder 1982). This ion signal S is given by

$$S = N_k \cdot P_{kI} \cdot \delta = N_i \cdot n_{L1} \cdot \sigma_{ik} \cdot \Delta x \cdot \frac{P_{kI}}{P_{kI} + R_k} \cdot \delta, \tag{2}$$

where N_i is the density of absorbing molecules, n_{L1} is the rate of incident laser photons of laser 1, P_{kI} the ionization rate of excited molecules in level $|k\rangle$, R_k the total relaxation rate of level $|k\rangle$ and δ is the detection probability of a photo-ion or electron. A tunable cw dye laser is used for the first step and a powerful argon ion laser for the second. The first transition $|i\rangle \rightarrow |\kappa\rangle$ can be generally saturated already at moderate laser powers while the second step has a much lower transition probability and requires therefore much higher laser powers in order to compete with the relaxation rate R_k. The transition probability of the second step becomes much larger, if the laser frequency ν_2 coincides with a transition to an autoionizing molecular Rydberg level (Schwarz *et al* 1988). In favorable cases a total detection sensitivity of 0·2–0·5 may be achieved. This means that every fifth to every second molecule in the absorbing level $|i\rangle$ can be detected!

3. Spectral resolution

The spectral resolution of molecular spectra measured in a collimated molecular beam is determined by several factors:

(a) The natural linewidth of the absorbing transition.
(b) A residual Doppler width which is determined by the collimation ratio $b/2d$, depending on the width b of the limiting aperture (for example the skimmer) and its distance d from the nozzle (see figure 1).
(c) Power broadening of the absorption lines, which is more severe in molecular beams than in cells because no collisions refill the lower level depleted by the laser absorption. Saturation is therefore reached at lower laser intensities.
(d) Transit time broadening in case of sharply focussed laser beams.
(e) Laser frequency jitter, which can be, however, reduced below 1 MHz by stabilization techniques.

Typical line widths achieved with moderate efforts are about 10 MHz, which is two orders of magnitude smaller than the Doppler width in cells at room temperature. Higher collimation ratios or the combination with Doppler-free nonlinear techniques yield line widths below 1 MHz if the natural line width is accordingly small (see § 7).

4. Cooling of molecules in supersonic beams

If a gas at a temperature T_0 expands from a reservoir with volume V_0 molecular density N_0 and pressure p_0 through a narrow hole (nozzle) into the vacuum, the rapid expansion results in a drastic adiabatic cooling of the gas. The internal energy $N_0 \cdot V_0 \cdot (f/2)kT_0$ of the molecules with f degrees of freedom in the reservoir and the potential energy $p_0 \cdot V_0$ is partly converted into directional flow energy of the gas.

The expanding gas can be collimated by a skimmer a few centimeters downstream of the nozzle (figure 1), thus forming a collimated beam. The distribution of molecular velocities $v_\parallel$ parallel to the molecular beam axis can often be approximated by a modified Maxwell distribution

$$N(v) = C \cdot v^{-2} \cdot e^{-(v-u/2KT_\parallel)}, \tag{3}$$

where u is the "flow velocity" of the expanded gas. From this distribution a "translational temperature" $T_\parallel$ can be deduced which describes the width of the velocity spread around the flow velocity u, and which can reach values down to 0·1 K (Toennies 1977).

From a molecular point of view the cooling of the gas proceeds via collisions during the expansion. Since the relative velocity $(\mathbf{v} - \mathbf{u})$ becomes very small, recombination of atoms or molecules to dimers and multimers can occur, i.e., clusters can be formed. Unfortunately, these recombination processes release their heat of formation which can again heat up the beam. In order to reduce these recombination processes, the gas under investigation is diluted at low concentrations in a nonreactive gas, called the carrier gas.

In such "seeded beams" the cooling is mostly achieved by the adiabatic expansion of the carrier gas. In order to produce "cold" molecular beams, the molecules under investigation are therefore mixed in a reservoir with the carrier gas, generally a noble gas, such as helium or argon, at pressures up to several bars. Typical molecular concentrations range from 0·1 to 10%. The gas mixture expands through a nozzle with diameters between 10–100 μm into the vacuum.

During the expansion the molecules can transfer, through collisions with the noble gas atoms, part of their internal energy (rotational and vibrational energy) into translational motion. If thermal equilibrium could be reached, all degrees of freedom (translational, rotational and vibrational) would reach the same low temperature. However, collisions can only occur within a short region (typically up to 10–30 nozzle diameters downstream) where the density is sufficiently high to allow collisions. The effectiveness of energy transfer depends on the number of collisions and on the deactivation cross-sections σ_{rot} for rotational-translational transfer and σ_{vib} for vibrational-translational or vibrational-rotational transfer. Since $\sigma_{vib} \ll \sigma_{rot}$ the vibrational cooling is much less effective than the rotational cooling and we obtain the

relation

$$T_{\text{trans}} < T_{\text{rot}} < T_{\text{vib}}.$$

Typical values of these different temperatures at 3 bar noble gas pressure are $T_{\text{trans}} \simeq 0{\cdot}5$ K, $T_{\text{rot}} \simeq 3$ K, $T_{\text{vib}} \simeq 50$–100 K, depending on the particular molecules and the noble gas. Helium generally yields lower rotational temperatures than argon.

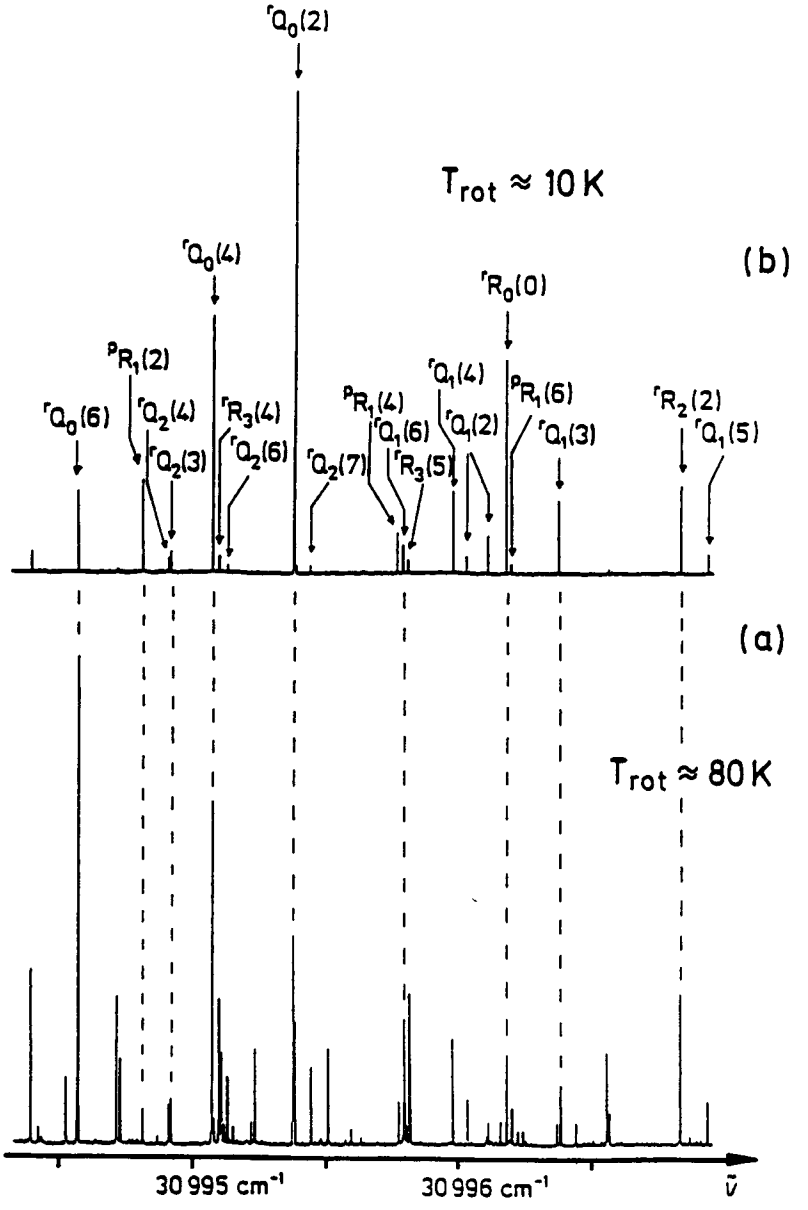

Figure 4. Section of a sub-Doppler excitation spectrum of the SO_2-molecule, (**a**) in a pure SO_2 beam at $T_{\text{rot}} \approx 80$ K, (**b**) in a supersonic argon beam, seeded with 5% SO_2 at $T_{\text{rot}} = 10$ K.

The low rotational temperatures T_{rot} result in a "compression" of the molecular population distribution $N(J)$ onto the lowest rotational levels with rotational quantum number J. Since the intensity of molecular absorption lines is proportional to the population $N(J)$ of the absorbing levels, the molecular spectrum is drastically simplified by this rotational cooling, because most of the lines in a spectrum taken at room temperature, disappear in the "cold spectrum". This is illustrated by figure 4, which shows a section of the absorption spectrum of SO_2 in a collimated molecular beam of pure $SO_2(T_{rot} \simeq 90\,K)$ and in a supersonic argon beam, seeded with 5% of $SO_2(T_{rot} \simeq 10\,K)$. One can clearly see that the intensities of lines from low rotational levels become larger with decreasing temperature T_{rot} while the lines from higher rotational levels disappear.

Pioneering work in the field of laser spectroscopy in cold free jets (without collimating slits) has been performed by Levy and coworkers (Levy *et al* 1977). Due to the low translational temperatures even loosely bound molecules, such as van der Waals molecules and clusters, can be efficiently formed and stabilized in cold supersonic beams (Levy 1980). This is now extensively used in many laboratories to study clüsters (see for instance Hagena 1984, Koenigstein Discussion Meeting 1984, Zū Pŭtlitz and Träger 1986, Jena *et al* 1987).

5. Nonlinear saturation spectroscopy in molecular beams

As was shown in § 2, the absorption lines have still a residual Doppler width, due to the finite collimation ratio of the molecular beam. In case of upper levels with long lifetimes τ the natural line width $\Delta\omega_n = 1/\tau$ may be much smaller than the residual Doppler width (example: $b/d = 50 \rightarrow \sin\epsilon = 0{\cdot}01 \rightarrow \Delta\omega_D^* = 2\pi \times 10^7\,s^{-1}$ with $\tau = 10^{-6}\,s \rightarrow \Delta\omega_n = 10^6\,s^{-1}$). Therefore the application of nonlinear techinques, such as saturation spectroscopy (Demtröder 1982), may yield a spectral resolution which exceeds the limit set by the residual Doppler width by more than one order of magnitude.

Saturation in nonlinear beams can be reached even at lower laser intensities than in cells since collisions are absent and the only mechanism, which refills the lower level, depleted by absorption of laser photons, is the flow of unpumped molecules into the interaction region. At low beam densities this flow is small and saturation of an allowed transition can be obtained even at laser intensities of a few mW/cm^2 (Demtröder 1989).

Some experiments on saturation spectroscopy in cold NO_2 beams (Bylicki *et al* 1989) illustrate the potential of this technique. The experimental arrangement is shown in figure 5. After having crossed the molecular beam, the laser beam is reflected back and crosses the molecular beam again under the same small angle ε as the first time, thus interacting with the same velocity group of molecules. When the laser frequency is tuned through an absorption line, a narrow Lamb-dip appears at the centre of the residual Doppler width (figure 6). If one of the beams is chopped and the excitation spectrum is monitored through a lock-in, turned to the chopping frequency, the linear part of the residual Doppler profile disappears and only the narrow part of the Lamb-dip appears (figure 6b).

The line widths of the Lamb-dips in the NO_2 spectrum are limited by frequency jitter of the stabilized dye laser and by transit time broadening. Due to the low

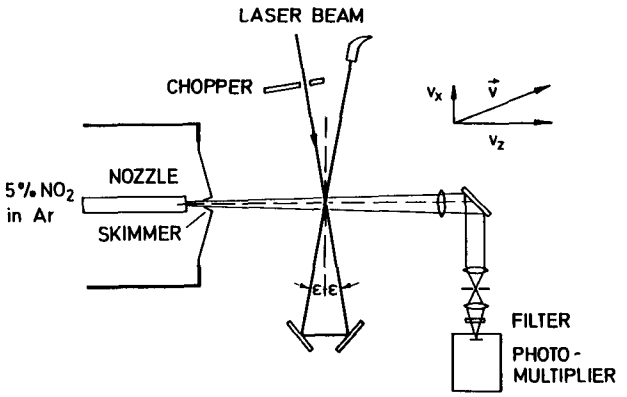

Figure 5. Experimental arrangement for Lamb-dip spectroscopy in a molecular beam.

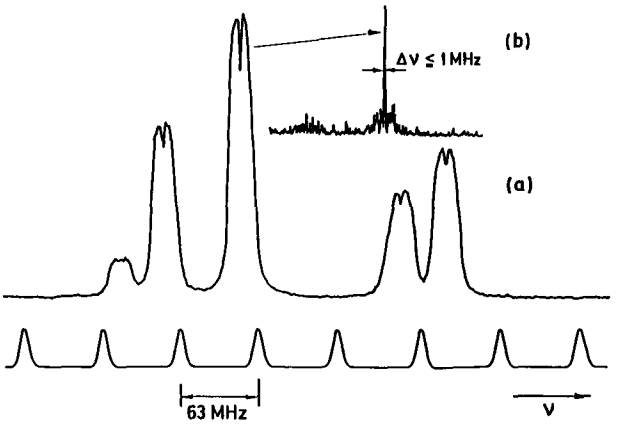

Figure 6. Lamb-dip spectrum of the *hfs*-components of a rotational transition in NO_2. The residual Doppler-width is about 10 MHz, the width of the Lamb-dip is < 1 MHz. (**a**) Without chopping the pump laser. (**b**) Elimination of Doppler background by lock-in detection at the chopping frequency of the pump beam.

saturation intensity, the laser beams must not be sharply focussed. This decreases the effect of transit time broadening and facilitates the alignment.

Recently similar experiments on Lamb-dip spectroscopy of radicals, such as OD and SiCl have been performed by Meijer *et al* (1987) which could resolve narrowly spaced hyperfine structure components, which were masked in the residual Doppler width of the linear spectra in a collimated beam.

6. Optical–optical double-resonance

Although the high spectral resolution achieved with the Lamb-dip technique allows the separation of even very narrowly spaced lines, the assignment of all these lines in a congested spectrum may still impose considerable difficulties. Here the optical–

optical double-resonance (OODR) method is very helpful, where a single mode laser L1 (called "pump-laser") is kept on a selected transition $|i\rangle \rightarrow |k\rangle$. When its beam is chopped at a frequency f_1, the populations of the two levels N_i and N_k, respectively, are modulated at f_1 with opposite phases. When a second laser L2 ("probe-laser") is tuned through the spectral range of interest, the absorption of L2 (monitored, for instance, by the laser-induced fluorescence) is modulated at f_1, if the laser frequency ω_2 coincides with a molecular transition starting from levels $|i\rangle$ or $|k\rangle$ (figure 7).

The application of OODR to molecular beam spectroscopy has the advantage of selective excitation of a single transition by the pump and accordingly unambiguous assignment of the modulated probe transitions. Figure 8 shows the experimental arrangement: The two parallel laser beams cross the molecular beam perpendicularly and are chopped at two different frequencies f_1 and f_2. The OODR-signals are then recorded at the sum frequency $f_1 + f_2$ which eliminates the Doppler-background.

Applied to the visible NO_2 spectrum the OODR technique allows the identification of all transitions starting from the same lower level $|i\rangle$ to closely lying upper levels $|m\rangle$ with the same rotational quantum numbers $|J, K\rangle$. These levels represent mutually perturbing rotational levels of different vibronic states. Since the density of

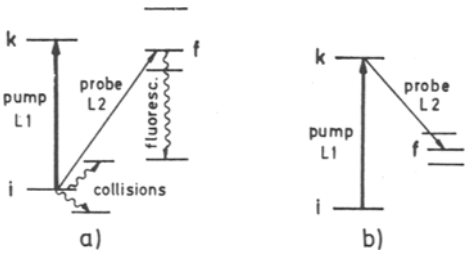

Figure 7. V-type OODR with common lower level $|i\rangle$ (**a**) and Λ-type OODR with a common upper level $|k\rangle$ (**b**) (Λ based on a stimulated resonance Raman process).

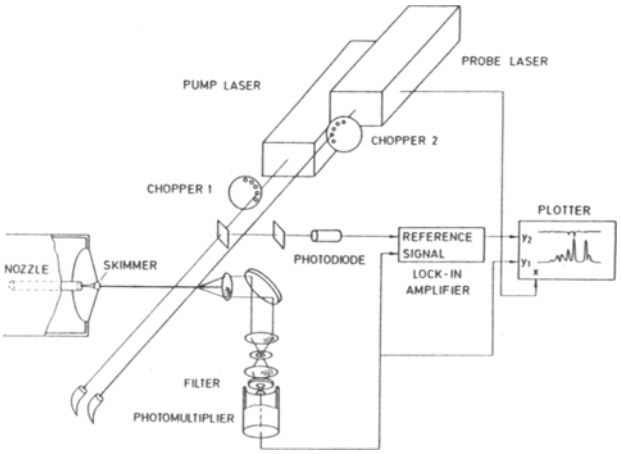

Figure 8. Experimental arrangement for OODR-spectroscopy in a collimated molecular beam.

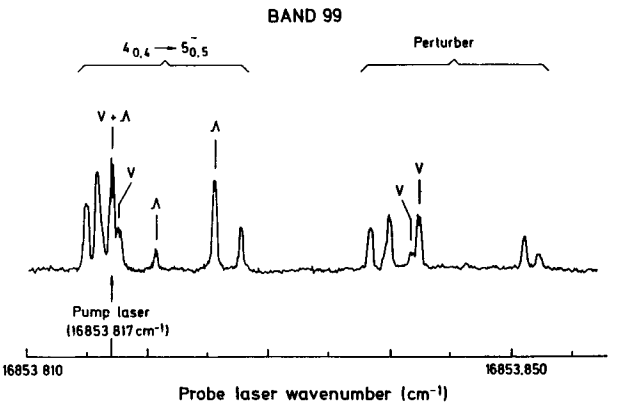

Figure 9. Coupled transitions in the NO_2 spectrum starting from a common lower level to pairs of mutually interacting upper levels.

directly accessible levels $|J'K'\rangle$ in the $^2B_2$ electronic states is much smaller than that of high lying vibronic levels of the $^2A_1$ electronic groundstate, each level $|J, K\rangle$ of the $^2B_2$ state may be perturbed by many levels of the $^2A_1$ state, where the degree of perturbation depends on the strength of the coupling matrix element and on the energy separation of the mutually perturbing levels.

Figure 9 shows for illustration a section of the high resolution spectrum of NO_2 where the pairs of transitions to mutually perturbing states has been assigned as a result of such OOD-measurements in a cold molecular beam.

7. Sub-Doppler laser spectroscopy of small metal clusters

Metal clusters M_n are bound systems of n metal atoms, which can be formed in a supersonic beam during adiabatic expansion by condensation of the metal vapor seeded in a noble gas (Hagena 1984). Their properties, such as binding energy, ionization potential, and geometrical structure depend on the kind but also on the number n of atoms forming the cluster. With increasing number n the ratio of "bulk" atoms inside the cluster to surface atoms increases and for large values of n the cluster should approach the properties of the solid state.

Many theoretical models have been proposed for the description of clusters, among which the "shell model" predicts maximum stability for closed shells with certain "magic numbers" n_m. Recent experiments on fragmentation of Na_n and K_n alkali clusters (Bréchignac *et al* 1987, 1988) have indeed proved that such magic numbers exist. However, the preferential fragmentation of clusters K_n after photoexcitation following, for all measured values of n, the scheme

$$K_n \rightarrow K_{n-1} + K \text{ or } K_n \rightarrow K_{n-2} + K_2$$

indicates that the excitation energy is more or less randomly distributed within the cluster, and the "evaporation" of atoms and dimers follows the dissociation paths of minimum energy of this statistical ensemble.

The geometrical structure of clusters can be inferred from rotationally resolved

spectra, while the stability against dissociation is related to the potential surfaces, obtained from vibrational analysis and from lifetime measurements and line profile determinations. The resolution of hyperfine structures gives information about the distribution of unpaired electrons over the locations of nuclei with nuclear spin. We will here illustrate some spectroscopic techniques used for the investigation of metal clusters by concentrating on sodium. The cluster size distribution $N(Na_n)$ in a supersonic argon beam seeded with Na vapor depends on various parameters, such as the oven temperature, the argon pressure, and the nozzle diameter and can be optimized within certain limits for the cluster Na_n under investigation (Delacretaz 1985).

The most extensive spectroscopic work has been performed so far on Na_3 (Fayet *et al* 1986; Broyer *et al* 1986a, b; Delacretaz 1985; Brechignae 1988; Lindsay 1976). With two pulsed lasers (the first is tuned through the electronic absorption bands and the second laser with fixed wavelength is used to ionize the excited molecules) the lowest excited electronic states have been measured for the first time by Wöste and his group (Broyer *et al* 1986) and could be compared with theoretical predictions. Because of the Jahn–Teller effect the minimum of the potential surface does not appear for the geometry of an equilateral triangle, as one might expect, but at an obtuse geometry. Figure 10 shows a low resolution scan of the visible absorption spectrum of Na_3 (Delacretaz 1985). A closer analysis of some bands shows that besides the vibrational structure a substructure appears which can be attributed to a pseudo-rotation of the molecular frame, where the Na-atoms tunnel through the shallow potential between three equivalent sites (Broyer *et al* 1986). The real rotational structure, caused by the rotation of the whole molecule, could, however, not be resolved in these experiments.

With single mode cw dye lasers the resolution can be greatly increased. This is demonstrated by figure 12 below, which shows a small section of the electronic band at $\lambda = 671$ nm, detected again by resonant two-photon ionization in the ion chamber of a quadrupole mass spectrometer. The many lines of this spectrum represent the partly resolved hyperfine structure and the rotational structure of Na_3. For a full resolution of all lines the width of 15 MHz, limited by power broadening, must be still decreased.

A comparison with a theoretical spectrum, based on *ab initio* calculations of the potential surfaces, shows that the contour of the Q-branch, shown in figure 11, is well reproduced. The individual lines, however, cannot be fitted by the theoretical model of a rigid asymmetric top, since pseudo-rotation and couplings between rotation and

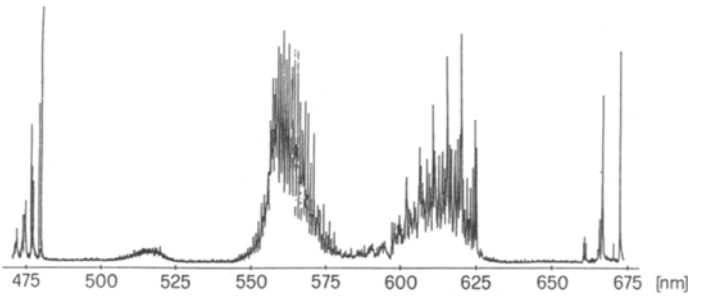

Figure 10. Low resolution scan of the visible absorption spectrum of Na_3 (Lindsay and Thompson 1982).

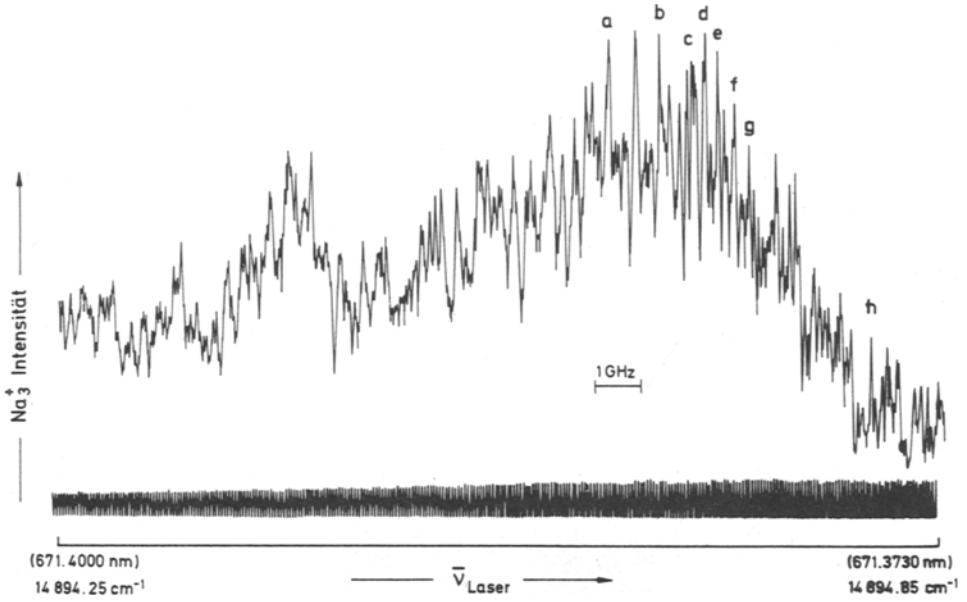

Figure 11. Sub-Doppler scan of a small section of the electronic band of figure 12 around $\lambda = 671$ nm.

vibration shift and split the lines. Since the analysis of such a complex spectrum is difficult, optical–optical double-resonance techniques have been used in order to simplify the spectrum. The experimental arrangement and the level scheme are shown in figure 12. A chopped single mode dye laser L1 is stabilized onto a selected transition $|i\rangle \rightarrow \delta k\rangle$ and depletes the lower level $|i\rangle$ partly. The resonant two-photon ionization spectrum, obtained with the tunable dye laser L2 for the first excitation step and an argon laser for the ionization, is now recorded through a lock-in, which is tuned to

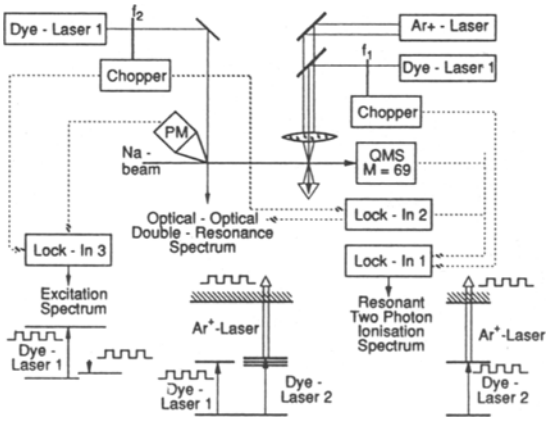

Figure 12. Experimental set-up for OODR-spectroscopy with two single mode dye lasers and an argon laser for the two-step photo-ionization of Na_3 in the ion chamber of a quadripol mass spectrometer.

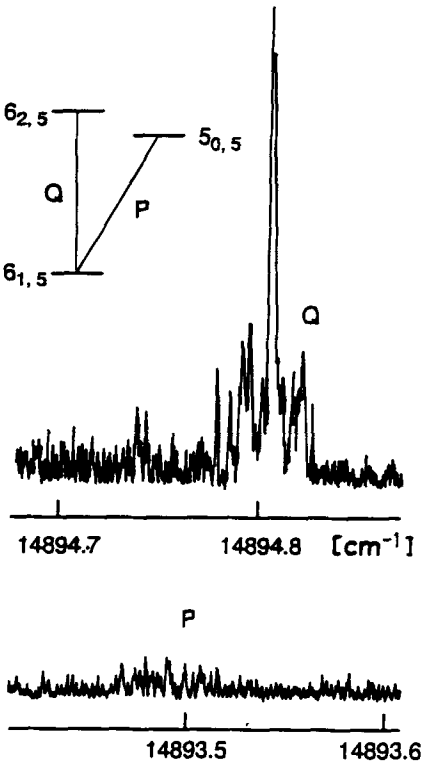

Figure 13. Hyperfine structure of a single rotational transition in Na_3, measured with OODR technique in a cold beam.

the chopping frequency of laser L1. The output signal of the lock-in, recorded as a function of the wavelength λ_2, contains only those transitions which start from the level $|i\rangle$, marked by L1. Such an optical–optical double resonance spectrum is shown in figure 13, where the pump laser was stabilized onto transition *b* in figure 11. The pattern represents an *hfs*-multiplet of a single rotational transition. The *hfs*-pattern can be satisfactorily explained if one assumes, in accordance with the results of Lindsay *et al* (1976) and Lindsay and Thompson (1982) obtained from electron spin resonance spectroscopy of Na_3 in a noble gas matrix, that the spin density, due to the unpaired electron, is unequally distributed over the three nuclei: only 8% at one nucleus but 46% at each of the two other nuclei.

The pseudo-rotation of the nuclei interchanges the role of the individual nucleus and therefore modifies the angular momentum coupling scheme and affects the rotational spectrum. More investigations are necessary to understand all fine details of this small but already complicated floppy molecule.

8. Conclusions

The examples, given in this paper, represent only a small selection of many investigations of molecules in cold beams by laser spectroscopy. They illustrate the

advantages and the limitations of these combined techniques. The rapid progress in this field has lead to an increasing area of applications, such as the study of large molecules of chemical or biological interest, investigations of seeding beams by absorptions of molecules from surfaces and also the study of molecular ions in cold beams. There is certainly still much to do in order to fully employ all experimental possibilities in this fascinating field.

References

Bréchignac C, Cabuzac Ph and Roux J Ph 1987 *J. Chem. Phys.* **87** 229

Bréchignac C, Cabuzac Ph and Roux J Ph 1988 *J. Chem. Phys.* **88** 3022

Bréchignac C, Cabuzac Ph, Roux J Ph, Pavolini D and Spiegelmann E 1987 *J. Chem. Phys.* **87** 5694

Bréchignac C, Cabuzac Ph, Roux J Ph, Pavolini D and Spiegelmann E 1988 *J. Chem. Phys.* **88** 3732

Broyer M, Delacretaz G, Labastie B, Whetten R L, Wolf J P and Wöste L 1986 *Z. Phys.* **D3** 131

Broyer M, Delacretaz G, Labastie P, Wolf J P and Wöste L 1986 *Phys. Rev. Lett.* **57** 1851

Bylicki F, Mehdizadeh E, Persch G and Demtröder W 1989 *Chem. Phys.* **135** 255

Delacretaz G 1985 *Proprietes Optique D'Aggregats Metallic En Phase Gazeüse*, Ph D thesis No 603, Ecole Polytechnique Federake de Lausanne

Demtröder W 1982 *Laser spectroscopy* (Heidelberg: Springer)

Demtröder W 1989 in *Visible and UV spectroscopy* (ed.) G Scoles *Atomic and molecular beam methods* (Oxford: University Press) vol. 2

Fayet P, Wolf J P and Wöste L 1986 *Phys. Rev.* **B33** 6792

Gottwald E 1985 PhD thesis, Fachbereich Physik, Universitat Kaiserslautern

Hagena O F 1984 *Rarified gas dynamics. Proc. 14th Int. Symp.* (ed.) H Oguch (Tokyo: University Press)

Jena P K, Rao B K and Khanna S V 1987 *Physics and chemistry of small clusters* (New York: Plenum)

Konigstein Discussion Meeting 1984 Experiments on clusters. *Ber Bunsenges Phys. Chem.* **88** 188–314

Levy D H 1980 in *Quantum dynamics of molecules* (ed.) R G Wooley (New York: Plenum Press)

Levy D H, Wharton L and Smalley R E 1977 in *Chemical and biochemical applications of lasers* (ed.) C B Moore (New York: Academic Press) vol. 2

Lindsay D M, Herschbach D R and Kwinam A L 1976 *Mol. Phys.* **32** 1199

Lindsay D M and Thompson G A 1982 *J. Chem. Phys.* **77** 1114

Meije G, Ubachs W, ten Meulen J J and Dynamus A 1987 *Chem. Phys. Lett.* **139** 603

Schwarz M, Duchowicz R, Demtröder W and Jungen Ch 1988 *J. Chem. Phys.* **89** 5460

Scholes G (ed.) 1988/1989 *Atomic and molecular beam methods* (Oxford: University Press) vols 1 and 2

Toennies J P and Winkelmann K 1977 *J. Chem. Phys.* **66** 3965

Zū Pütlitz G and Träger F (eds) 1986 Conference on metal clusters, Heidelberg *Z. Phys.* **D2** 100